Journal of Engineering Mathematics **38:** 427–438, 2000.

Diffusion-controlled smoulder propagation in a composite slab

J. ADLER
Department of Mathematics, Imperial College of Science Technology and Medicine, London SW7 2BZ, United Kingdom

Received 8 June 1999; accepted in revised form 26 April 2000

Abstract. The steady propagation of a thin smouldering front parallel to the faces of a composite reactive slab has been considered. The slab consists of a double layer of solid with differing densities. As the smouldering front progresses into the solid it leaves behind an inert porous medium through which oxidizer is able to diffuse to the front. It is assumed that the reactive solid is sufficiently dense for no oxidizer to be present. The oxidizer concentration on one face of the slab is specified, the other being impervious to the transport of reactants. Dimensionless equations and boundary conditions are obtained for the concentration of oxidizer in the porous medium. These are solved to first order by use of a complex-variable method and a hodograph transformation giving the shape of the smouldering front for various parameter combinations. The analysis is extended to the case where the layers are of unequal thickness. Simple expressions for the shape of the front and the oxidizer concentration are obtained when one layer thickness is large. The model here considered is a first step in a more comprehensive analysis of smouldering in a non-uniform medium.

Key words: smoulder propagation, diffusion control, double layer

1. Introduction

Smouldering is a combustion process that lies between the extremes of negligible exothermic reaction and flame-like burning. Such process is usually controlled by the rate at which oxidizer is able to reach the combustion zone. Smouldering leaves a porous solid remainder through which the oxidizer is able to pass by diffusion, convection or both.

Although smouldering is a complicated physical and chemical process (see Drysdale [1]), it can be represented by the progression of a thin reaction front through a solid which is sustained by oxidizer diffusion from a bounding surface (see Ohlemiller [2]). There is considerable experimental evidence that such a model is physically realistic (see Beever [3]).

An asymptotic theory of steady smouldering in a half-space has been considered previously by Adler and Herbert [4]. Here a thin reaction zone propagates parallel to a plane surface on which a constant oxidizer concentration is maintained. The solid fuel into which this zone propagates is assumed to be sufficiently dense for no oxidizer to be present. To first order, the shape of the reaction front is found to be parabolic, a consequence of the condition at the front where the concentration of oxidizer vanishes and where the rate of oxidizer supply balances the rate at which solid fuel is being consumed. The paper of Adler and Herbert contains references to earlier studies of smouldering and to related work.

The theoretical problem of smouldering in a semi-infinite solid fuel gives rise to a free-boundary problem, namely, the position of the reaction from must be determined as part of the solution. Kerr [5], has devised a numerical scheme for obtaining the shape of this front

and the oxidizer concentration behind it. The work also considers other plane surface oxidizer concentrations and confirms the previous theoretical analysis [4].

The previous papers [4, 5] have only been concerned with the oxidizer concentration behind the front. The asymptotic temperature distribution has been determined by Herbert, Kerr and Adler [6]. The technique used was to integrate the equations for temperature and oxidizer concentration across the smouldering front to obtain jump conditions which relate the changes in these quantities to the assumed strength of the line heat sources on the front. The asymptotic temperature distribution is then found from the known oxidizer distribution.

The experimental work of Ohlemiller on polyurethane foam has shown that smouldering can result in a significant volume loss. In addition, the properties of the surface of the burnt material, specifically the surface mass-transfer coefficient for air at this surface, may be expected to be of importance in determining the shape of the front and the distribution of oxidizer behind it. Both these effects have been taken account of in Herbert, Kerr and Adler [7] in which the surface of the burnt material is assumed to be of parabolic form.

Previous work has been concerned with asymptotic properties with no information as to what happens where the smouldering front meets the plane surface. By using suitable coordinate transformations, Adler and Herbert [8] investigated this region. One outcome is to show the existence of 'upstream influence', namely, the oxidizer concentration at the plane surface is no longer discontinuous but changes smoothly from its zero value on the front to its constant value on the plane surface. This is analogous to the bending of the concentration profiles as determined experimentally by Ohlemiller.

For smouldering in a semi-infinite region, the reduction of the conservation equation and boundary conditions for the oxidizer results in a single dimensionless parameter. This is generally small since it contains the ratio of a gas to solid density. When a finite-thickness region, such as slab geometry is considered, a further dimensionless group appears which contains the thickness of the slab. A most useful parameter is the Peclet number, which is also of the same order of magnitude, since it contains a small smoulder-propagation speed. Measured values of u' are typically 10^{-3} cm s^{-1}. For finite regions an added complication is that more boundary conditions have to be satisfied, in particular, if oxidizer diffuses through opposite parallel surfaces [9].

A different approach to the smouldering problem is contained in the work of Buckmaster [10]. He considers a shallow wave with a finite steadily moving region of surface oxidizer flux and solves the corresponding Dirichlet problem. The solution is then used in the differential condition for the wave front to determine its shape. The thermal problem for slab smoulder with free-stream convection is also considered. A comparison with the model to be presented below is given in Section 5.1.

Previous theoretical approaches have been concerned with propagation through a uniform reactive solid. It is known that smouldering often occurs through non-uniform materials, *e.g.* earth-fill sites, peat, etc., or composite layered media having different physical and chemical properties. Below, we consider steady propagation parallel to the surfaces of a double-layered solid in which the reaction front is sustained by oxidizer diffusion through one of the bounding surfaces. As in previous work a simple kinetic scheme has been considered, namely, fuel + oxidizer $\rightarrow$ porous solid + gases with the appropriate oxidizer diffusivity within the porous medium.

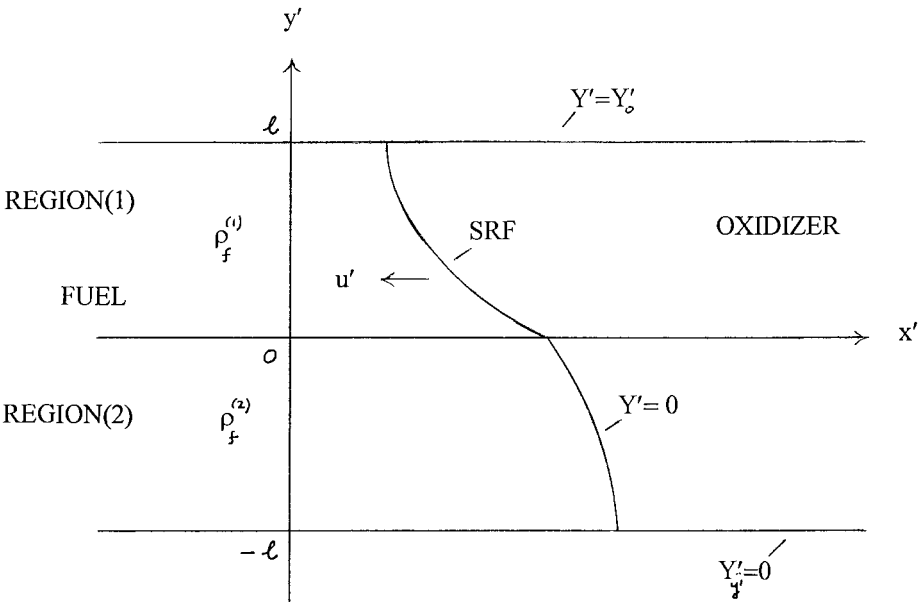

Figure 1. Double layered solid with smouldering reaction front (SRF) propagating in the negative x' direction.

2. Conservation equations

Consider the steady propagation of a thin smouldering reaction front (SRF) through a double layer $-\ell \leq y' \leq \ell$ of solid reactive material, with density $\rho_f^{(1)}$ in $0 \leq y' \leq \ell$ and $\rho_f^{(2)}$ in $-\ell \leq y' \leq 0$. Oxidizer is assumed to diffuse from $y' = \ell$ to the front which propagates at a constant speed u' parallel to the plane surfaces, see Figure 1. The conservation equation for the concentration of oxidizer may be written in terms of coordinates relative to the moving front. We assume that the oxidizer concentration on the SRF vanishes and that the unreacted solid is sufficiently dense for no oxidizer to be present. Let the two regions be denoted by (1) and (2). Suitable dimensionless equations for the oxidizer $Y(x, y)$ in the inert porous regions behind the front are then:

Medium (1):

$$\begin{aligned} p\frac{\partial Y}{\partial x} &= \frac{\partial^2 Y}{\partial x^2} + \frac{\partial^2 Y}{\partial y^2}, \quad 0 < y < 1, \\ Y(x, 1) &= 1, \quad x > x_1, \\ \frac{\partial Y}{\partial y}(x, 1) &= 0, \quad x < x_1, \end{aligned} \tag{1}$$

SRF conditions:

$$p\frac{\mathrm{d}y}{\mathrm{d}x} = s_1\left(\frac{-\partial Y}{\partial y} + \frac{\partial Y}{\partial x}\frac{\mathrm{d}y}{\mathrm{d}x}\right), \quad Y = 0. \tag{2}$$

Medium (2):

$$\begin{aligned} p\frac{\partial Y}{\partial x} &= \frac{\partial^2 Y}{\partial x^2} + \frac{\partial^2 Y}{\partial y^2}, \quad -1 < y < 0, \\ \frac{\partial Y}{\partial y}(x, -1) &= 0, \quad x > x_2, \end{aligned} \tag{3}$$

SRF conditions:

$$p\frac{\mathrm{d}y}{\mathrm{d}x} = s_2\left(\frac{-\partial Y}{\partial y} + \frac{\partial Y}{\partial x}\frac{\mathrm{d}y}{\mathrm{d}x}\right), \quad Y = 0. \tag{4}$$

Conditions (2) and (4) state that oxidizer diffusion at the front balances the rate of consumption of solid reactant.

In the above equations the dimensionless variables are given by

$$\begin{aligned} x &= (x' + u't')/\ell, \quad y = y'/\ell, \quad Y = Y'/Y_0', \\ p &= \ell u'/D, \quad s_i = (\rho_0/\rho_f^{(\mathrm{i})})(Y_0'/n_0), \end{aligned} \tag{5}$$

where x', y' are Cartesian coordinates, t' is the time, Y_0' is the fractional surface concentration of oxidizer whose mean density is ρ_0, D is the diffusivity and n_0 is the stoichiometric coefficient for the solid fuel/oxidizer reaction. In (1) and (3) x_1 and x_2 are constants to be determined.

Smouldering speeds are typically $u' \sim 10^{-3}$ cm s^{-1}, [1], and the constants s_i in (5) are small due to the density ratio $\rho_0/\rho_f^{(\mathrm{i})}$. Values depend on the material, but typically $s_i \sim 10^{-2}$. For a 2 cm thickness slab and reasonable values for D, the Peclet number is $p \sim 10^{-1}$.

3. A first-order problem

We now expand $Y(x, y)$ as a power series in the Peclet number p and set $s_i = p/\lambda_i$, $i = 1, 2$ where λ_i are constants. The terms independent of p in the two regions then satisfy
Medium (1):

$$\nabla^2 Y = 0, \quad 0 < y < 1, \tag{6}$$

SRF:

$$\lambda_1\frac{\mathrm{d}y}{\mathrm{d}x} = \frac{-\partial Y}{\partial y} + \frac{\partial Y}{\partial x}\frac{\mathrm{d}y}{\mathrm{d}x}, \quad Y = 0, \tag{7}$$

Medium (2):

$$\nabla^2 Y = 0, \quad -1 < y < 0, \tag{8}$$

SRF:

$$\lambda_2\frac{\mathrm{d}y}{\mathrm{d}x} = \frac{-\partial Y}{\partial y} + \frac{\partial Y}{\partial x}\frac{\mathrm{d}y}{\mathrm{d}x}, \quad Y = 0, \tag{9}$$

where

$$\nabla^2 = \frac{\partial^2}{\partial x^2} + \frac{\partial^2}{\partial y^2}.$$

We note that, although $Y(x, y)$ satisfies the two-dimensional Laplace equation, the coordinates x, y are in a frame moving with the smoulder front. We now introduce the complex conjugate $Z(x, y)$ of this function which will be found useful in determining a solution. The Cauchy-Riemann conditions for the two functions are

$$\frac{\partial Y}{\partial x} = \frac{\partial Z}{\partial y}, \quad \frac{\partial Y}{\partial y} = -\frac{\partial Z}{\partial x}.$$

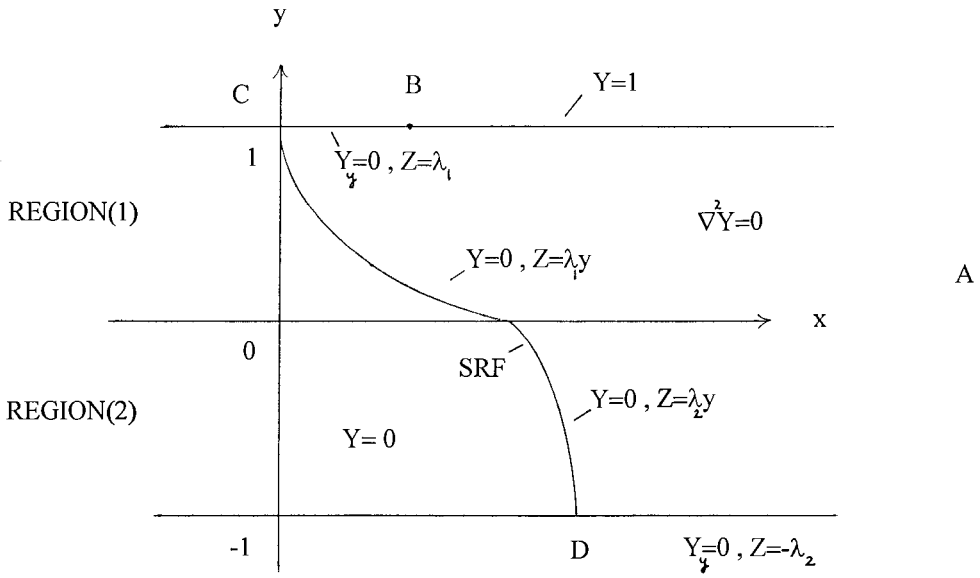

Figure 2. Boundary values on Y and Z in (x, y) plane.

From (7) and (9)

$$\lambda_i \mathrm{d}y = \frac{\partial Z}{\partial x}\mathrm{d}x + \frac{\partial Z}{\partial y}\mathrm{d}y, \quad i = 1, 2,$$

and hence

$$\frac{\partial}{\partial x}(Z - \lambda_i y)\mathrm{d}x + \frac{\partial}{\partial y}(Z - \lambda_i y)\,\mathrm{d}y = 0.$$

If $Z = 0$ when $y = 0$, it follows that $Z = \lambda_i y$ on the SRF. Let $\mathrm{d}s = (\mathrm{d}x, \mathrm{d}y)$ and $\mathrm{d}n = (\mathrm{d}y, -\mathrm{d}x)$ be line elements along and perpendicular to the SRF. The oxidizer flux through the smouldering front is

$$\int_{y=-1}^{y=1} \frac{\partial y}{\partial n}\mathrm{d}s = \int_{y=-1}^{y=1} \frac{\partial Z}{\partial s}\mathrm{d}s = Z|_{y=1} - Z|_{y=-1} = \lambda_1 + \lambda_2. \tag{10}$$

Values of $Y(x, y)$ and $Z(x, y)$ on the boundaries are shown in Figure 2. There is a region on $y = 1$, behind the front, at which $\partial Y/\partial y = 0$. Previous work has shown that this is due to 'upstream influence' [8, 9].

A solution to Equations (6)–(9) may be obtained by interchanging the roles of dependent and independent variables. The domain in the hodograph plane in which a solution to $\nabla^2 y = 0$ is sought is shown in Figure 3, as are the relevant boundary values of $y(Y, Z)$. The required solution is

$$y = Z/\lambda_i + Y(1 - Z/\lambda_i) + \sum_{n=1}^{\infty} B_n \sin(n\pi Y) \sinh n\pi(\lambda_1 - Z), \tag{11}$$

where

$$B_n = 4(-1)^n/[n\pi \sinh n\pi(\lambda_1 + \lambda_2)].$$

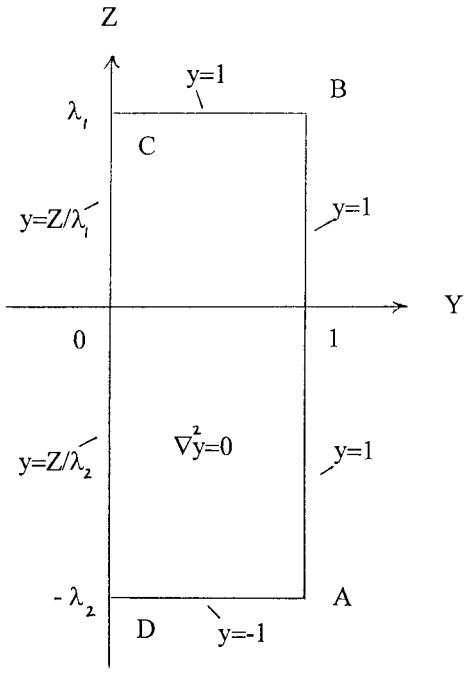

Figure 3. Boundary values on y in (Y, Z) plane.

An expression for $x(Y, Z)$ can be found from the Cauchy-Riemann conditions $\partial x/\partial Y = \partial y/\partial Z$, $\partial x/\partial Z = -\partial y/\partial Y$ and integration.
The results is

$$x = -Y^2/(2\lambda_i) + Z^2/(2\lambda_i) + Y/\lambda_i - Z + B_0 + \sum_{n=1}^{\infty} B_n \cos(n\pi Y) \cosh n\pi(\lambda_1 - Z), \tag{12}$$

where B_0 is a constant.
On the SRF, $Y = 0$, $Z = \lambda_i y$ where $i = 1, 2$, hence the equation of the front is

$$x = \frac{1}{2}\lambda_i y^2 - \lambda_i y + B_0 + \sum_{n=1}^{\infty} B_n \cosh[n\pi(\lambda_1 - \lambda_i y)]. \tag{13}$$

If this passes through $x = 0$, $y = 1$, $(i = 1)$, then

$$B_0 = \frac{1}{2}\lambda_1 - \sum_{n=1}^{\infty} B_n.$$

On $y = 1$, $Y(x, 1) = 1$ for $x \geq x_B$ where x_B is found by setting $Y = 1$, $Z = \lambda_1$ in (12). Thus

$$x_B = \frac{1}{2\lambda_1} + \sum_{n=1}^{\infty}[(-1)^n - 1]B_n. \tag{14}$$

Since Y and Z are complex conjugates, Y=const. and Z=const. form a mutually orthogonal system. Thus Z=const. leaves the SRF ($Y = 0$) at rightangles with Z able to take the values

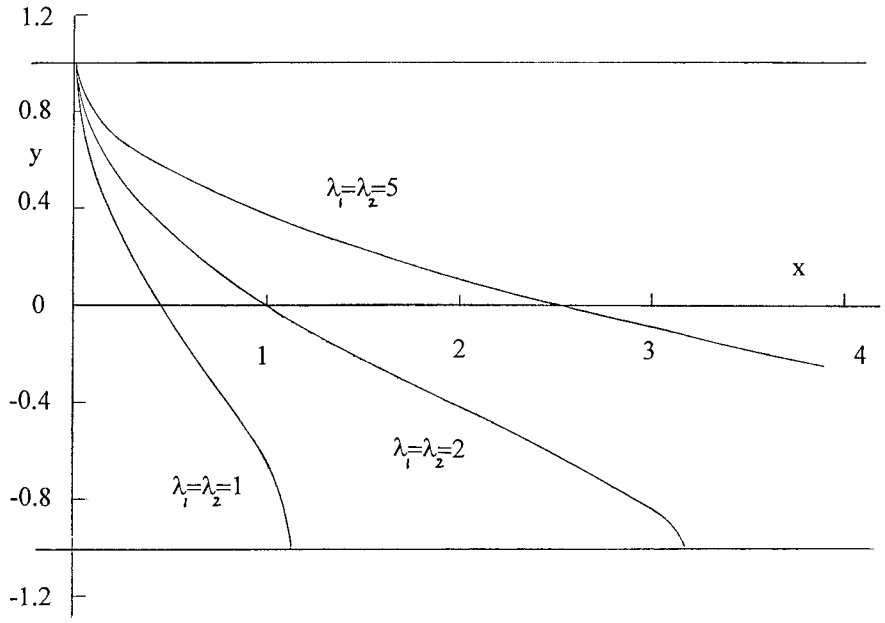

Figure 4. Shape of the SRF for $\lambda_1 = \lambda_2 = 1, 2, 5$.

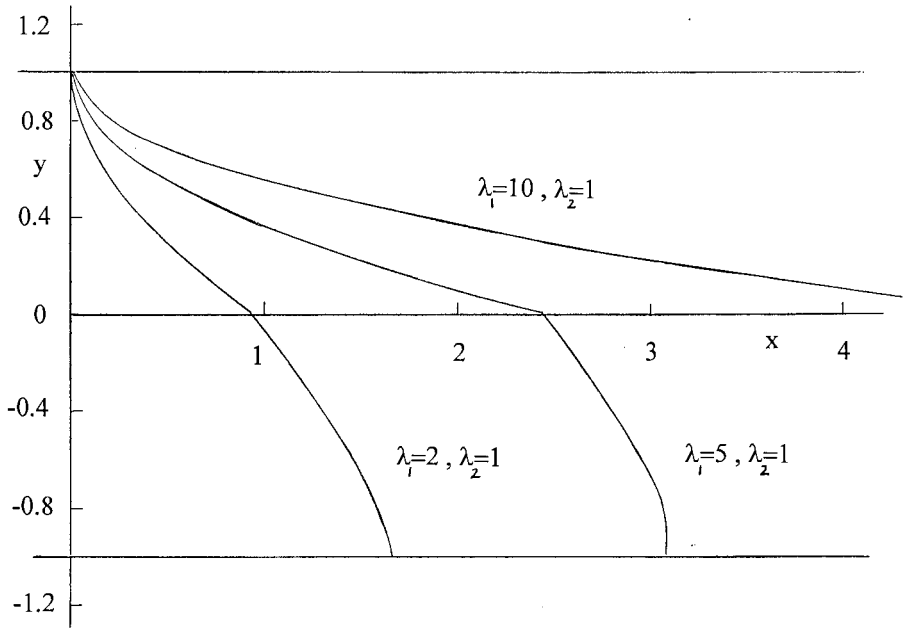

Figure 5. Shape of the SRF for $\lambda_1 = 2, 5, 10$ and $\lambda_2 = 1$.

$-\lambda_2 \leq Z \leq \lambda_1$. Iso-concentration surfaces for a fixed Y can be obtained from (11) and (12) by varying Z. The shape of the SRF, to first order, for various λ_i has been calculated from Equation (13); the results are shown in Figures 4–6.

The analysis above assumes for simplicity that the slab layers are of equal thickness; the case of unequal layers is discussed below. By definition $\lambda_i = (\ell u' \rho_f^{(i)} n_0)/(D\rho_0 Y_0')$, where $i = 1, 2$ refers to the upper and lower layer, respectively, and $\rho_f^{(i)}$ is the corresponding un-

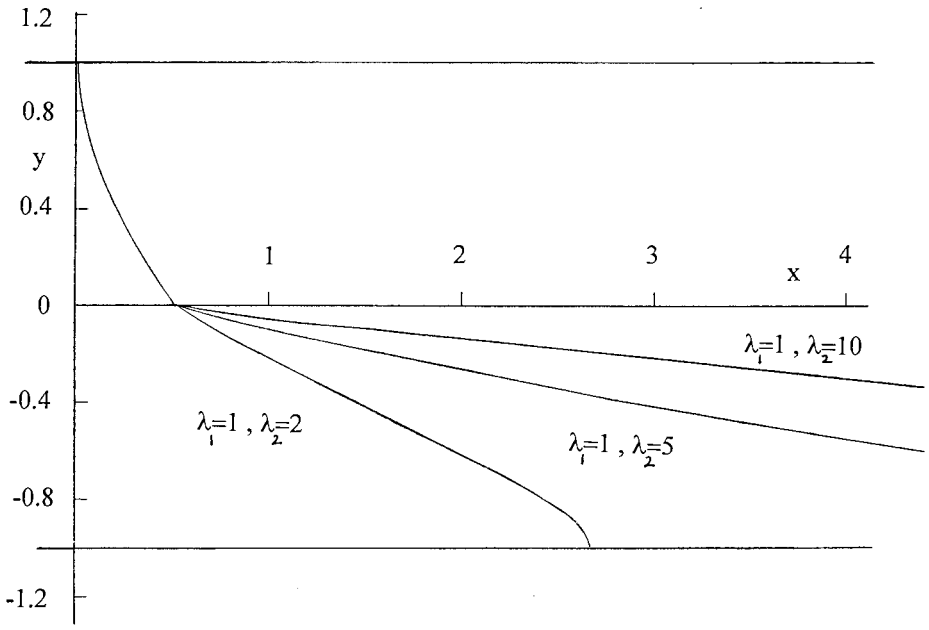

Figure 6. Shape of the SRF for $\lambda_1 = 1$ and $\lambda_2 = 2, 5, 10$.

reacted fuel concentration. In Figure 4 both fuel concentrations are equal, the shape of the smouldering front being stretched with increasing λ_i, in particular as the speed of smoulder increases. Figure 5 shows how the shape of the front varies with increasing upper-layer fuel concentration when that of the lower layer is fixed. In Figure 6 the alternative assumption is made, namely, the lower-layer concentration varies. We note that, due to the change of fuel concentrations in Figures 5, 6, the shape of the front is discontinuous on $y = 0$. Somer further comments regarding Figures 4, 5, 6 are given in the discussion section.

4. Layers of unequal thickness

Let region (1) be $0 \le y' \le \ell$ and region (2) be $-\ell' \le y' \le 0$. The problem in the hodograph plane is now similar to that considered previously but with changed boundary values. We have

$$\nabla^2 y = 0,$$

where

$$\begin{array}{llll} y = 1 & \text{when } Z = \lambda_1, & 0 \le Y \le 1, & \\ y = -y_0 & \text{when } Z = -\lambda_2 y_0, & 0 \le Y \le 1, & \\ y = Z/\lambda_1 & \text{when } Y = 0, & 0 \le Z \le \lambda_1, & (15) \\ y = Z/\lambda_2 & \text{when } Y = 0, & -\lambda_2 y_0 \le Z \le 0, & \\ y = 1 & \text{when } Y = 1, & -\lambda_2 y_0 \le Z \le \lambda_1, & \end{array}$$

where

$$y_0 = \ell'/\ell.$$

The solution of problem (15) is

$$y = Z/\lambda_i + Y(1 - Z/\lambda_i) + \sum_{n=1}^{\infty} \tilde{B}_n \sin(n\pi Y) \sinh n\pi(\lambda_1 - Z), \tag{16}$$

where

$$\tilde{B}_n = 2(-1)^n(1 + y_0)/[n\pi \sinh n\pi(\lambda_1 + \lambda_2 y_0)].$$

The function $x(Y, Z)$, obtained from the Cauchy-Riemann conditions, is

$$x = -\frac{1}{2}Y^2/\lambda_i + \frac{1}{2}Z^2/\lambda_i + Y/\lambda_i - Z + \frac{1}{2}\lambda_1 + \\ + \sum_{n=1}^{\infty} \tilde{B}_n[\cos(n\pi Y)\cosh(n\pi(\lambda_1 - Z)) - 1]. \tag{17}$$

The equation of the SRF is here

$$x = \frac{1}{2}\lambda_i y^2 - \lambda_i y + \frac{1}{2}\lambda_1 + \sum_{n=1}^{\infty} \tilde{B}_n[\cosh(n\pi(\lambda_1 - \lambda_i y)) - 1]. \tag{18}$$

Below we examine some particular cases.

5. Some particular cases

5.1. The case $y_0 \to 0$

For $y_0 \to 0$ the problem reduces to smoulder propagation in a uniform slab of thickness ℓ with a specified oxidizer concentration on one surface and insulation on the other. The result for $y_0 \to 0$ also gives the symmetric solution in a half-slab of twice the thickness with oxidizer diffusion through both plane surfaces.

For $\ell' \to 0$, ℓ finite, the functions Y, Z are given parametrically by

$$y = Z/\lambda_1 + Y(1 - Z/\lambda_1) + \sum_{n=1}^{\infty} \hat{B}_n \sin(n\pi Y)\sinh n\pi(\lambda_1 - Z) \tag{19}$$

$$x = -\frac{1}{2}Y^2/\lambda_1 + \frac{1}{2}Z^2/\lambda_1 + Y/\lambda_1 - Z + \frac{1}{2}\lambda_1 + \\ + \sum_{n=1}^{\infty} \hat{B}_n[\cos(n\pi Y)\cosh(n\pi(\lambda_1 - Z)) - 1]. \tag{20}$$

where

$$\hat{B}_n = 2(-1)^n/[n\pi \sinh(n\pi\lambda_1)].$$

The equation of the SRF becomes

$$x = \frac{1}{2}\lambda_1(1 - y)^2 + \sum_{n=1}^{\infty} \hat{B}_n[\cosh n\pi\lambda_1(1 - y) - 1] \tag{21}$$

and this meets the x-axis where

$$x = x_0 = \frac{1}{2}\lambda_1 + \sum_{n=1}^{\infty} \hat{B}_n[\cosh n\pi\lambda_1 - 1] \\ = \frac{1}{2}\lambda_1 + 2\sum_{n=1}^{\infty}(-1)^n \tanh\left(\frac{1}{2}n\pi\lambda_1\right)/(n\pi). \tag{22}$$

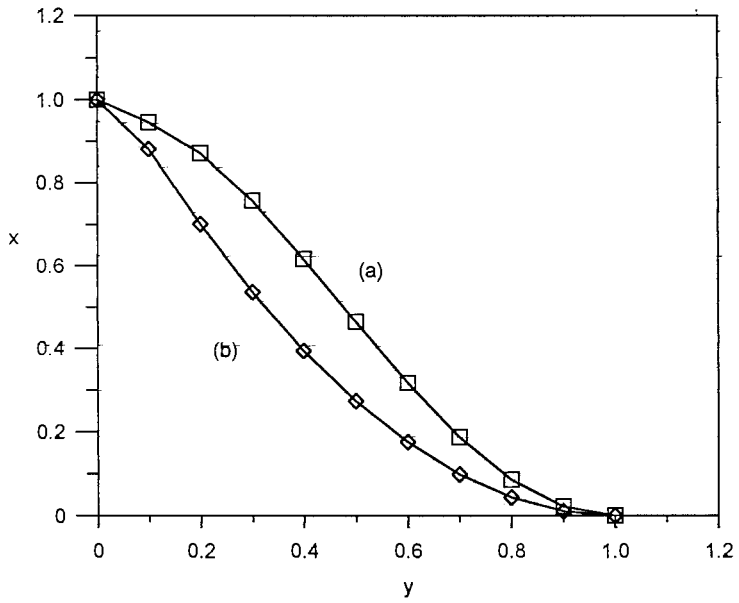

Figure 7. Normalised shape of the SRF for a single layer of solid ($\ell' = 0$) when (a) $\lambda_1 = 1$, (b) $\lambda_1 = 10$.

In the smouldering model of Buckmaster [10], the oxidizer concentration at the surface vanishes over a finite strip, the remaining surface being impermeable (Equations 14a–c). He defines a Peclet number

$$\mathrm{Pe}_{\mathrm{Buck}} = uH/D = \mathrm{Pe}H/\ell \tag{23}$$

where $\mathrm{Pe} = \ell u/D$ is the definition used in our paper. In (23) H is the wavelength of a shallow smouldering wave and $\mathrm{Pe}_{\mathrm{Buck}}$ is taken to be of order unity.

In order to compare Buckmaster's results with ours, the normalised shapes of the smouldering fronts for $\lambda_1 = 1, 10$ have been evaluated from (21) and (22). These are shown in Figure 7 and are seen to be similar to those of Figure 4 of Buckmaster's paper.

5.2. THE CASE $Y_0 \to \infty$

Some simplification arises when $y_0 \to \infty$ since then $\tilde{B}_n \to 0$. Here (16) and (17) can be written as

$$y = 1 - (1 - Y)(1 - Z/\lambda_i), \tag{24}$$

$$x = -(1 - Y)^2/(2\lambda_i) + \frac{\lambda_i}{2}(1 - Z/\lambda_i)^2 + 1/(2\lambda_i) - \frac{1}{2}\lambda_i + \frac{1}{2}\lambda_1,$$

and the equation of the SRF is

$$x = \frac{1}{2}\lambda_i(1 - y)^2 + \frac{1}{2}\lambda_1 - \frac{1}{2}\lambda_i. \tag{25}$$

Equations (24) may be solved for $Y(x, y)$. When $i = 1$, corresponding to the finite-thickness layer,

$$Y(x, y) = 1 - \lambda_1^{\frac{1}{2}}[\{(x - 1/(2\lambda_1))^2 + (1 - y)^2\}^{\frac{1}{2}} - x + 1/(2\lambda_1)]^{\frac{1}{2}} \tag{26}$$

which is the result (4.16) of [9].

In (26) there is a branch-point at $x_B = 1/(2\lambda_1)$, $y = 1$, and $Y(x, 1) = 1$ for $x \geq x_B$. $Y(x, 1)$ increases from zero to one in the range $0 \leq x \leq x_B$.

6. Conclusions

Our analysis assumes that the propagation speed u' is a known constant. In general, this must be determined by considering the thermodynamics, chemical kinetics and material properties in a finite reaction zone. An analysis of this type is contained in the work of Schult *et al.* [13] in which oxidizer is supplied by forced convention, the gas flow and smoulder propagation being in the same direction. In smoulder with natural convection (see Schult *et al.* [14]) oxidizer flows through a porous solid to the reaction front in the opposite direction to that of the propagating front. The paper contains an analysis of the stability of the combustion wave using both asymptotic methods and direct numerical computation. In practice, the smouldering process is flexible enough to adapt to a wide range of oxygen supply levels. Because of this flexibility smoulder suppression is surprisingly difficult.

The initiation of smouldering can be defined in terms of turning-point bifurcations in a suitable parameter space (see Brindley, Jivra, Merkin and Scott [11, 12]). These bifurcations lie between those defining the quiescent state and flaming combustion.

Although the analysis above has only been carried out to first order in the Peclet number, the solutions possess features which are in accord with observation. The upstream influence, in which the bounding concentration varies smoothly between its plane surface value $Y = 1$ and that at the smoulder front corresponds to a folding of the reaction zone, although in practice one would have a smooth continuous surface within the porous residue. In principle, it is possible to extend our analysis to higher order in the Peclet number, but the nature of the solutions would make this difficult. An exception is the case $y_0 \to \infty$ for which higher order results have previously been found [9]. A possible procedure is to assume that the shape of the front is given by the first-order problem and then obtain the next term in the expansion for Y. The shape of the front can then be corrected with the amended value of Y.

Computed shapes of the smouldering fronts for various combinations of λ_i are shown in Figures 4, 5, 6. When $\lambda_1 \not\equiv \lambda_2$ the gradients on $y = 0$ are discontinuous due to the change in fuel concentration. By definition

$$\lambda_i = p/s_i = (\ell u' \rho_f^{(i)} n_0)/(D \rho_0 Y_0'), \tag{27}$$

so that $\lambda_1 > \lambda_2$ corresponds to an upper layer richer in combustible than the lower one. For fixed λ_1, changes in λ_2 have little influence on the shape in Region (1), this being approximately

$$x = \frac{1}{2}\lambda_1(1 - y)^2. \tag{28}$$

The result of Equation (10) confirms that $\lambda_1 + \lambda_2$ is the dimensionless oxidizer flux through the SRF and hence through the plane surface $y = 1$.

In order to suppress smouldering it is important to bring the reaction front as close to the bounding surface as possible. Figure 5 shows that this occurs with increasing λ_1, although the reaction front is stretched in the x-direction. The fire engineering implications are that sharp changes in fuel concentration are easier to deal with than slowly changing ones.

For $y_0 \to 0$ our analysis reduces to smouldering in a uniform layer. A similar mathematical problem arises in the continuous casting of a slab from a pool of molten metal (see Siegel [15]) where solutions in terms of elliptic integrals have been obtained.

References

1. D.D. Drysdale, Aspects of smouldering combustion. *Fire Prevention Science and Technology* 23 (1981) 18–28.
2. T.J. Ohlemiller, Smouldering combustion hazards of thermal insulation materials. U.S. Department of Commerce, Report NBSIR 81–2350 (1981).
3. P.F. Beever, *Initiation and Propagation of Smouldering Reactions*. Ph.D. thesis, University of Leeds (1986) 305 p.
4. J. Adler and D.M. Herbert, Diffusion controlled smoulder propagation parallel to a plane surface. *SIAM J. Appl. Math.* 52 (1992) 153–162.
5. C.E. Kerr, Diffusion-controlled smoulder propagation in a semi-infinite solid: A numerical solution. *IMA. J. Appl. Math.* 48 (1992) 149–162.
6. D.M. Herbert, C.E. Kerr and J. Adler, Diffusion-controlled smoulder propagation in a semi-infinite solid: The asymptotic temperature distribution. *IMA J. Appl. Math.* 53 (1994) 127–136.
7. D.M. Herbert, C.E. Kerr and J. Adler, Diffusion-controlled smouldering combustion with material shrinkage. *Q. J. Mech. Appl. Math.* 47 (1994) 43–52.
8. J. Adler and D.M. Herbert, Nonplanar smoulder propagation governed by diffusion. *IMA J. Appl. Math.* 61 (1998) 105–117.
9. J. Adler, Diffusion controlled smoulder propagation in a thin slab. *J. Eng. Math.* 30 (1996) 527–545.
10. J. Buckmaster, A theory of shallow smoulder waves. *IMA J. Appl. Math.* 56 (1996) 87–102.
11. J. Brindley, N.A. Jivra, J.H. Merkin and S.K. Scott, Stationary state solutions for coupled reaction-diffusion and temperature-conduction equations I: Infinite slab and cylinder with general boundary conditions. *Proc. R. Soc. London* A430 (1990) 459–477.
12. J. Brindley, N.A. Jivra, J.H. Merkin and S.K. Scott, Stationary state solutions for coupled reaction-diffusion and temperature-conduction equations II: Spherical geometry with Dirichlet boundary conditions. *Proc. R. Soc. London* A430 (1990) 479–488.
13. D.A. Schult, B.J. Matkowsky, V.A. Volpert and A.C. Fernandez-Pello, Forced forward smolder combustion. *Combust. Flame 104* (1996) 1–26.
14. D.A. Schult, A. Bayliss and B.J. Matkowsky, Travelling waves in natural counterflow filtration combustion and their stability. *SIAM J. Appl. Math.* 58 (1998) 806–852.
15. R. Siegel, Analysis of solidification interface shape during continuous casting of a slab. *Int. J. Heat Mass Transfer* 21 (1978) 1421–1430.